

## Plane-strain bulge test for nanocrystalline copper thin films

Xiaoding Wei,<sup>a,b,\*</sup> Dongyun Lee,<sup>c</sup> Sanghoon Shim,<sup>d</sup> Xi Chen<sup>a,e</sup> and Jeffrey W. Kysar<sup>a,b</sup>

<sup>a</sup>Columbia Nanomechanics Research Center, Columbia University, New York, NY 10027, United States

<sup>b</sup>Department of Mechanical Engineering, Columbia University, New York, NY 10027, United States

<sup>c</sup>Korea Institute of Science and Technology, Materials Science and Technology Division, 39-1, Hawolgok-dong, Seongbuk-gu, Seoul 136-791, South Korea

<sup>d</sup>Division of Materials Science and Technology, Oak Ridge National Laboratory, Oak Ridge, TN 37831, United States

<sup>e</sup>Department of Civil Engineering and Engineering Mechanics, Columbia University, New York, NY 10027, United States

Received 23 February 2007; revised 27 April 2007; accepted 8 May 2007

Available online 18 June 2007

Free-standing nanocrystalline Cu films with grain size around 39 nm are fabricated by thermal evaporation and characterized by the plane-strain bulge test. Young's modulus and yield stress at a 0.2% offset are about 110–130 GPa and 400 MPa, respectively. Results show that the strength of the n-Cu films is largely independent of film thickness at a strain rate less than  $10^{-5} \text{ s}^{-1}$ . No grain growth is observed and the predominant plastic deformation mechanism is grain boundary sliding accompanied by dislocation mechanisms. © 2007 Acta Materialia Inc. Published by Elsevier Ltd. All rights reserved.

**Keywords:** Nanocrystalline materials; Thin films; Bulge test

Nanocrystalline materials, with average grain size less than 100 nm have been of interest since their introduction in 1984 [1,2] because of a broad range of potential applications [3,4] based upon their enhanced mechanical properties (such as higher strength and hardness) as compared to their coarse-grained counterparts. As reviewed in [2], the most common preparation techniques for nanocrystalline metals and alloys are inert gas condensation (IGC) [5,6], ball milling [7,8] and pulsed electroplating [9,10], etc. In order to fulfill their potential, the mechanical properties of nanocrystalline materials need to be understood as a function of both the grain size and the feature dimension (e.g. film thickness).

Compression, uniaxial tensile and indentation tests have been performed on both bulk [6,11–15] and micron scale nanocrystalline metals [16–25]. The results show that the material's strength generally increases when grain size becomes smaller as per the Hall–Petch effect, although Chokshi et al. [26], Conrad and Narayan [27] observed an inverse Hall–Petch relationship in indentation experiments when the material's grain size is smaller than a critical value.

In the present study, nanocrystalline copper (n-Cu) thin films are synthesized by thermal evaporation and the mechanical properties are explored using the “plane-strain bulge test” introduced by Vlassak and Nix [28]. The results are compared to previously published studies on the mechanical properties of similar free standing thin films with a micrometer grain size [29] and with nanometer grain size [23].

The n-Cu films are prepared by thermal evaporation (Edwards Auto 306 Vacuum Evaporator). The base pressure in the chamber is  $1 \times 10^{-6}$  Torr and high purity (99.995%) Cu is evaporated onto a specially prepared substrate from a tungsten boat 120 mm below. A current of 2.4 A is applied through the tungsten boat to melt the Cu source which yields a deposition rate of 0.1–0.2 nm/s. During the process, the substrate temperature is no higher than 70 °C.

The fabrication procedure is modified from that of Xiang et al. [30]. A (100) Si wafer with a 500 nm thick  $\text{Si}_3\text{N}_4$  layer deposited on both sides by low pressure chemical vapor deposition (LPCVD) is used. Positive photo-resist AZ5214 (CLARIANT), ultraviolet photolithography (wavelength of 365 nm) and reactive ion etching (RIE, 250 mTorr, 250 W in  $\text{CF}_4/\text{O}_2$  atmosphere, TECHNICS Series 800) is employed to open a rectangular window through the  $\text{Si}_3\text{N}_4$  on one side of the wafer. Next, the Si wafer is anisotropically etched in 30 wt.% potassium hydroxide (KOH) solution at 80 °C

\* Corresponding author. Address: Department of Mechanical Engineering, Columbia University, New York, NY 10027, United States. Tel.: +1 212 853 8515; fax: +1 212 854 3304; e-mail: [wx2102@columbia.edu](mailto:wx2102@columbia.edu)

until a free standing rectangular  $\text{Si}_3\text{N}_4$  membrane remains on the opposite side of the wafer. The n-Cu is then deposited on the  $\text{Si}_3\text{N}_4$  membrane by thermal evaporation and another RIE etching with lower pressure and power (150 mTorr and 150 W) is used to remove the  $\text{Si}_3\text{N}_4$ , so that a freestanding n-Cu film is obtained; since the copper film is exposed to the plasma for only a short time after the  $\text{Si}_3\text{N}_4$  has been etched away, the RIE procedure is not expected to significantly modify the material properties of the Cu film. Inspection of the film surface with SEM did not show any observable defects. All processes after depositing the n-Cu are done at the room temperature, in order to encourage stability of grain size.

A scanning electron microscope (SEM) micrograph in Figure 1a shows the grains on the film surface. The grain size on the surface is characterized by drawing four lines across the image center and defining the intercepts of grain boundaries as grain size. The distribution histogram shown in Figure 1b indicates the most prevalent surface grain size to be in the range of 40 nm. In addition, X-ray diffraction (XRD) studies are also performed to analyze the grain size of the n-Cu films (Inel XRD 3000 module, Cu  $K\alpha$ ). The XRD pattern of the 180 nm thick n-Cu film is shown in Figure 2a. Average grain size is estimated by the Williamson–Hall method [31] as shown in Figure 2b, which leads to an average grain size of between 36 nm and 41 nm for different specimens. The specimen thicknesses (measured by Dektak Profilometer) and average grain sizes obtained by both methods are listed in the Table 1. Similar XRD measurements taken two weeks after deposition show no evidence of grain growth.

The ratios of integral intensity of peaks (200), (220) and (311) to peak (111) are, respectively, 34.0%, 13.2% and 10.2%. By comparing those values to that of standard powder provided by the International Centre for Diffraction Data (ICDD) [32], the specimens show a slight (111) texture. In addition, since during deposition, the homologous temperature,  $T_s/T_m$ , was less than

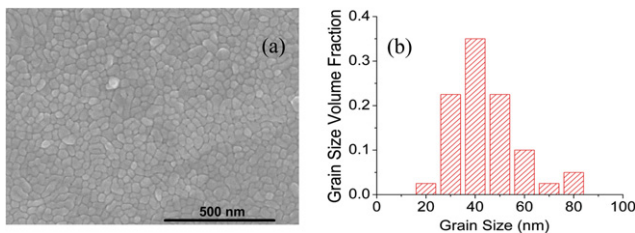


**Figure 1.** (a) SEM image of the 180 nm n-Cu film; (b) Grain size distribution of the n-Cu film calculated from the SEM image.

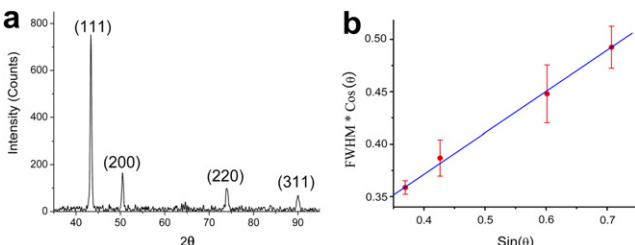


**Figure 2.** (a) The X-ray diffraction pattern of the 180 nm n-Cu film; (b) the Williamson–Hall plot from the XRD pattern of the n-Cu film.

**Table 1.** Film thickness,  $t$ , average grain size of films from XRD and SEM, Young's moduli and yield stresses

Sample	$t$ (nm)	$D_{\text{XRD}}$ (nm)	$D_{\text{SEM}}$ (nm)	$E$ (GPa)	$\sigma_y$ (MPa)
No. 1	173	37	$38 \pm 5$	$130 \pm 5$	$395 \pm 5$
No. 2	180	38	$38 \pm 4$	$132 \pm 5$	$404 \pm 2$
No. 3	220	38	$39 \pm 5$	$111 \pm 7$	$425 \pm 3$
No. 4	428	38	$39 \pm 7$	$129 \pm 6$	$410 \pm 1$
No. 5	476	40	$41 \pm 6$	$131 \pm 5$	$365 \pm 5$
No. 6	998	42	$41 \pm 5$	$120 \pm 5$	$360 \pm 5$

0.25, ( $T_s$  is the substrate temperature, and  $T_m$  is the melting temperature of Cu [33]), the film is expected to consist of very fine equiaxed grains [34,35].

The bulge tests were initiated within one hour after the end of the film preparation. During the thin film bulge test, a compressed air source with electronic pressure regulator is used to control the pressure applied on the film to maintain a strain rate of about  $5 \times 10^{-6} \text{ s}^{-1}$ . The pressure,  $p$ , is recorded with a resolution of 0.05 kPa and a laser interferometer measures the out-of-plane deflection,  $h$ , at the center of the film with a resolution of 316.5 nm. The film thickness is denoted as  $t$ , and the film width and length ( $2.5 \times 14 \text{ mm}$ ) are denoted, respectively, as  $2a$  and  $2b$ . Xiang et al. [30] showed that for rectangular membranes with aspect ratio greater than four, the stress state at the middle part of the membrane is close to plane strain which allows straightforward analysis of the data. Since  $t \ll 2a$  and  $t \ll h$ , the edges of the free-standing film can be treated as plastic hinges. Assuming the shape of the deformed film away from the ends to be that of a circular arc, the in-plane stress,  $\sigma$ , and strain,  $\varepsilon$ , in the width direction of the film can be written as [30]

$$\sigma = \frac{pa^2}{2ht} \quad \text{and} \quad \varepsilon = \frac{2h^2}{3a^2}, \quad (1)$$

when  $h \ll 2a$ . The stress and strain given by Eq. (1) is the plane-strain behavior of the n-Cu film. From the unloading curve, the plane-strain modulus,  $M$ , can be obtained; subsequently, Young's modulus of the material,  $E$ , is determined as  $M(1 - \nu^2)$ , where  $\nu$  is the Poisson's ratio for the bulk material; taken [33] to be 0.35.

Figure 3a shows the plane-strain stress–strain curves for the six n-Cu films examined and three curves of the coarse-grained Cu films from [29] are also included for comparison. Young's moduli of the n-Cu films, compiled in Table 1, are in the range of 111–132 GPa, in good agreement with published values [33] and also within the range defined by the Reuss and Voigt bounds [36] of about 109 GPa and 144 GPa, respectively.

In typical coarse-grained materials, the yield stress  $\sigma_y$  is often defined with a 0.2% strain offset. However, it has been reported [37] that a more appropriate strain offset level for nanocrystalline metals is as high as 0.7% in order to ensure that plastic deformation occurs in nearly all grains. In present study, due to the loss of ductility, the films did not reach that strain level. Therefore the yield stress values are reported in Table 1 at 0.2% strain offset, however it is emphasized that not all grains may have deformed plastically at this strain level. To demonstrate the behavior of the films past the 0.2% strain

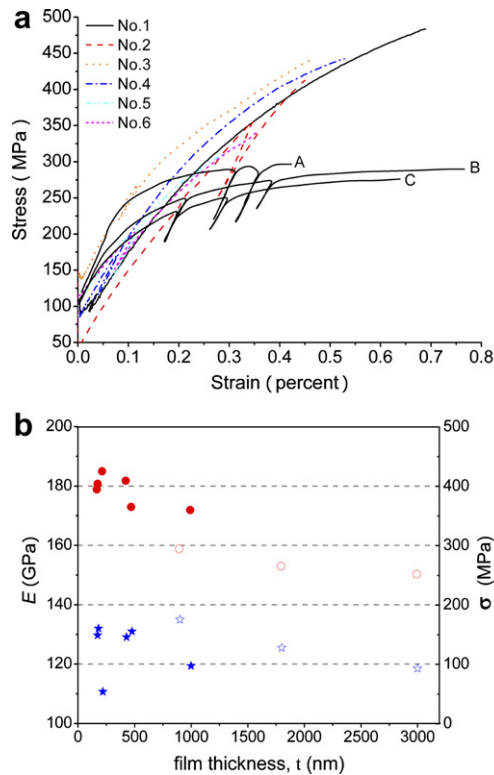


**Figure 3.** (a) The plane-strain stress–strain curves of the six n-Cu films with different thickness. Results of the coarse-grained Cu films from [29] are also included for comparison: curves A, B and C are films with thickness of 0.9, 1.8 and 3.0 μm, and the grain size is about 1.8–1.9 μm. (b) Summary of Young's moduli (star symbol) and yield stresses (round symbol) with different film thickness. The solid symbols are data for n-Cu films and the open symbols are for coarse-grained Cu films from [29].

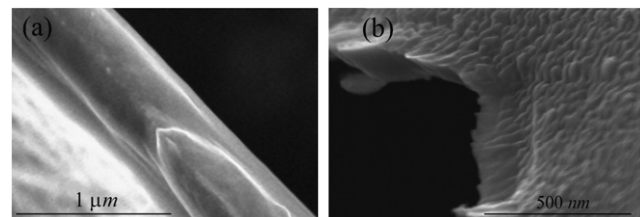
offset, it can be observed that specimen No. 1 in Figure 3b failed at an offset strain of about 0.4%, at a stress of 482 MPa rather than the 395 MPa at 0.2% offset strain, approximately a 25% increase.

Figure 3b compares results from the n-Cu films with those of coarse-grained (about 1.85 μm) Cu films deposited via electrodeposition and characterized with a bulge test by Xiang et al. [29]. The Cu films in [29] were synthesized by electro-deposition and had a dominant  $\langle 111 \rangle$  texture. In addition, although the average grain size of the films in [29] was on the order of micrometers, the authors reported evidence of twins with a spacing of about 500 nm which could have served to inhibit dislocation motion and increase the material strength. Nevertheless, the grain size of the Cu films in the present study is at least one order of magnitude smaller than the twin spacing in the coarse-grained films. The yield stress at 0.2% strain offset of the n-Cu films is significantly higher than that of the coarse-grained Cu films. Also the yield stress of the coarse-grained Cu films from [29] is dependent on film thickness; in particular the yield stress increases with decreasing film thickness due to the inherently smaller grains of the thinner films [29,38,39].

There does not seem to be a pronounced thickness dependence of the yield stress for the n-Cu films as there is for the coarse-grained films at the strain rate of  $5 \times 10^{-6} \text{ s}^{-1}$ . Although the two thicker specimens, No. 5 and No. 6 have a yield stress level of about

365 MPa, all other specimens show a consistent range of  $410 \pm 10$  MPa. Such a conclusion is reasonable because the grain size of those films is much smaller than the order of the film thicknesses. As shown in Figure 3a, the n-Cu films can achieve a ultimate stress of about 450 MPa, which is 50% higher than that of the coarse-grained Cu, 300 MPa, reported in [29]. Moreover, the results show that the n-Cu has less macroscopic ductility than the coarse-grained thin films and there is no obvious yield point in the data of Figure 3a.

The process by which the ultimate failure occurs in the n-Cu films depends upon the location relative to the edge of the free standing film. Figure 4 shows evidence of shear localization from a portion of the film away from the edges. The permanent deformation which led to failure was clearly dominated by grain boundary sliding as evident by the granular structure visible on the sheared surface in Figure 4b; however it is likely that the grains themselves deformed via dislocation mechanisms in order to accommodate the grain boundary sliding. Figure 5a shows the progression of a crack-like feature near the edge of the free standing film. The actual zone of the failure extends over several micrometers, even though the film thickness is less than 1 μm. A closer view in Figure 5b shows an uplift of material near the tip consistent with a Mode III ripping behavior. There is again evidence of grain boundary sliding, however close inspection reveals a series of highly planar strain localizations which pass through several grains parallel to the Mode III crack tip which suggests the possibility of dislocation activity. Thus, grain boundary sliding appears to be the predominant deformation mechanism, with some evidence of dislocation activity associated with near crack tip plasticity. The deformation mechanisms associated with both types of failure are consistent with studies [40,41], which state the deformation mechanism in n-Cu with grain sizes of those in the present experiments are thought to be grain boundary sliding accompanied by dislocation mediated plasticity within the nanoscale grains to accommodate grain boundary sliding.



**Figure 4.** (a) Knife-edge fracture surface of the n-Cu film; (b) Shear failure surface caused by intergranular shear.

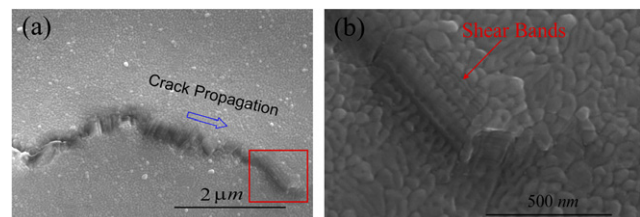


**Figure 5.** (a) SEM image of Mode III crack tip of the n-Cu film; (b) Highlighted region from (a) showing shear bands in front of the crack tip which suggest shear localization.

Finally, it is of interest to compare the thin film bulge test with the results of tensile tests of free standing nanocrystalline metal films [23] in which two classes of stress-strain response are reported. One class was for films which had been deposited using sputter deposition at a vacuum of  $10^{-6}$  Torr, which exhibited a high yield stress, and limited ductility due to shear localization which occurred at a very low level of plastic strain. The other class of response was for films which had been deposited under vacuum conditions of  $10^{-7}$  Torr. This response was characterized by a distinct yielding behavior at significantly lower stress levels followed by very little hardening with failure occurring at much larger strains. The authors [23] show that the differences in response can be attributed to an effective absence of grain growth in specimens with the first response and stress-assisted grain growth in the specimens with the second response. They suggest that the difference can be explained based upon impurities deposited at the grain boundaries in the poorer vacuum level. While a different deposition method was used in the present set of experiments, the same vacuum level ( $10^{-6}$  Torr) was used as for the first class of response in [23], and the resulting mechanical response is quite similar. That combined with an absence of perceptible grain growth in our specimens suggests that impurities in the grain boundaries tend to pin grain boundaries to limit grain growth just as in [23,42].

Supports from NSF DMR-0650555, NSF CMMI-0500239, from the Academic Quality Fund of Columbia University, and NSF CMS-0407743, are gratefully acknowledged. In addition, this work was supported in part by the MRSEC Program of the National Science Foundation under Award Number DMR-0213574 and by the New York State Office of Science, Technology and Academic Research (NYSTAR). The authors also thank Prof. J. Vlassak and his research group for very helpful discussions.

- [1] R. Birringer, H. Gleiter, H.P. Klein, P. Marquardt, *Physics Letters A* 102 (1984) 365–369.
- [2] H. Gleiter, *Progress in Materials Science* 33 (1989) 223–315.
- [3] A. Inoue, *Materials Science and Engineering A-Structural Materials Properties Microstructure and Processing* 304 (2001) 1–10.
- [4] R. Schulz, J. Huot, G. Liang, S. Boily, G. Lalande, M.C. Denis, J.P. Dodelet, *Materials Science and Engineering A* 267 (1999) 240–245.
- [5] G.W. Nieman, J.R. Weertman, R.W. Siegel, *Scripta Metallurgica* 23 (1989) 2013–2018.
- [6] J.R. Weertman, *Materials Science and Engineering A* 166 (1993) 161–167.
- [7] H.J. Fecht, E. Hellstern, Z. Fu, W.L. Johnson, *Metallurgical Transactions A-Physical Metallurgy and Materials Science* 21 (1990) 2333–2337.
- [8] D. Oleszak, P.H. Shingu, *Journal of Applied Physics* 79 (1996) 2975–2980.
- [9] U. Erb, *Nanostructured Materials* 6 (1995) 533–538.
- [10] H. Natter, R. Hempelmann, *Journal of Physical Chemistry* 100 (1996) 19525–19532.
- [11] G.W. Nieman, J.R. Weertman, R.W. Siegel, *Scripta Metallurgica Et Materialia* 24 (1990) 145–150.
- [12] V.Y. Gertsman, M. Hoffmann, H. Gleiter, R. Birringer, *Acta Metallurgica Et Materialia* 42 (1994) 3539–3544.
- [13] P.G. Sanders, J.A. Eastman, J.R. Weertman, *Acta Materialia* 45 (1997) 4019–4025.
- [14] C.J. Youngdahl, P.G. Sanders, J.A. Eastman, J.R. Weertman, *Scripta Materialia* 37 (1997) 809–813.
- [15] K.M. Youssef, R.O. Scattergood, K.L. Murty, J.A. Horton, C.C. Koch, *Applied Physics Letters* 87 (2005).
- [16] M. Legros, B.R. Elliott, M.N. Rittner, J.R. Weertman, K.J. Hemker, *Philosophical Magazine A-Physics of Condensed Matter Structure Defects and Mechanical Properties* 80 (2000) 1017–1026.
- [17] R.D. Emery, G.L. Povirk, *Acta Materialia* 51 (2003) 2079–2087.
- [18] Y.M. Wang, K. Wang, D. Pan, K. Lu, K.J. Hemker, E. Ma, *Scripta Materialia* 48 (2003) 1581–1586.
- [19] Z. Budrovic, H. Van Swygenhoven, P.M. Derlet, S. Van Petegem, B. Schmitt, *Science* 304 (2004) 273–276.
- [20] Y.M. Wang, S. Cheng, Q.M. Wei, E. Ma, T.G. Nieh, A. Hamza, *Scripta Materialia* 51 (2004) 1023–1028.
- [21] Y.M. Wang, E. Ma, *Materials Science and Engineering A-Structural Materials Properties Microstructure and Processing* 375–377 (2004) 46–52.
- [22] D.Y.W. Yu, F. Spaepen, *Journal of Applied Physics* 95 (2004) 2991–2997.
- [23] D.S. Gianola, S. Van Petegem, M. Legros, S. Brandstetter, H. Van Swygenhoven, K.J. Hemker, *Acta Materialia* 54 (2006) 2253–2263.
- [24] D.S. Gianola, D.H. Warner, J.F. Molinari, K.J. Hemker, *Scripta Materialia* 55 (2006) 649–652.
- [25] M. Verdier, H. Huang, F. Spaepen, J.D. Embury, H. Kung, *Philosophical Magazine* 86 (2006) 5009–5016.
- [26] A.H. Chokshi, A. Rosen, J. Karch, H. Gleiter, *Scripta Metallurgica* 23 (1989) 1679–1683.
- [27] H. Conrad, J. Narayan, *Applied Physics Letters* 81 (2002) 2241–2243.
- [28] J.J. Vlassak, W.D. Nix, *Journal of Materials Research* 7 (1992) 3242–3249.
- [29] Y. Xiang, T.Y. Tsui, J.J. Vlassak, *Journal of Materials Research* 21 (2006) 1607–1618.
- [30] Y. Xiang, X. Chen, J.J. Vlassak, *Journal of Materials Research* 20 (2005) 2360–2370.
- [31] G.K. Williamson, W.H. Hall, *Acta Metallurgica* 1 (1953) 22–31.
- [32] I. International Centre for Diffraction Data, Title from back of container: Powder diffraction file: PDF-4/full file, Newtown Square, Pa.: International Centre for Diffraction Data, 2002.
- [33] A. International, *Metals Handbook*, Materials Park, Ohio, ASM International, 1990, pp. 1110–1114.
- [34] J.A. Thornton, *Annual Review of Materials Science* 7 (1977) 239–260.
- [35] C.R.M. Grovenor, H.T.G. Hentzell, D.A. Smith, *Acta Metallurgica* 32 (1984) 773–781.
- [36] R. Hill, *Proceedings of the Physical Society of London Section A* 65 (1952) 349–355.
- [37] S. Brandstetter, H. Van Swygenhoven, S. Van Petegem, B. Schmitt, R. Maass, P.M. Derlet, *Advanced Materials* 18 (2006) 1545–1548.
- [38] Y. Xiang, J.J. Vlassak, *Scripta Materialia* 53 (2005) 177–182.
- [39] L. Nicola, Y. Xiang, J.J. Vlassak, E. Van der Giessen, A. Needleman, *Journal of the Mechanics and Physics of Solids* 54 (2006) 2089–2110.
- [40] H. Conrad, *Metallurgical and Materials Transactions A-Physical Metallurgy and Materials Science* 35A (2004) 2681–2695.
- [41] M.A. Meyers, A. Mishra, D.J. Benson, *Progress in Materials Science* 51 (2006) 427–556.
- [42] M.A. Haque, M.T.A. Saif, *Proceedings of the National Academy of Sciences of the United States of America* 101 (2004) 6335–6340.